

The virial mode k_v approach to Structure Formation with Warm Dark Matter

Axel de la Macorra ^{a,b,1} and Jorge Mastache ^{c,d}

^aInstituto de Física, Universidad Nacional Autónoma de México, Circuito de la Investigación Científica Ciudad Universitaria, 04510, CDMX, México.

^bInstituto de Ciencias del Cosmos, University of Barcelona, ICCUB, Barcelona 08028, Spain.

^cMesoamerican Centre for Theoretical Physics, Universidad Autónoma de Chiapas, Carretera Zapata Km. 4, Real del Bosque, 29040, Tuxtla Gutiérrez, Chiapas, México.

^dConsejo Nacional de Ciencia y Tecnología, Av. Insurgentes Sur 1582, Colonia Crédito Constructor, Del. Benito Juárez, 03940, Ciudad de México, México

E-mail: macorra@fisica.unam.mx, a.macorra@gmail.com, jhmastache@mctp.mx

Abstract. The small scale structure opens a window to constrain the dynamical properties of Dark Matter. Here we study the clustering of warm dark matter (WDM) in a semi-analytical approach and compared the linear power spectrum of WDM with cold dark matter (CDM) employing a new transfer function $T_v(a, k)$ in terms of the virial wave number $k_v = 2\pi/\lambda_v$ corresponding to a structure with a virial radius $r_v = \lambda_v/2$, half the size of the free streaming scale radius $r_v = r_{fs}/2 = \lambda_{fs}/4$. The virial mass M_v contained in this structure corresponds to the lightest structure formed for a WDM particle becoming non-relativistic at the scale factor a_{nr} with the corresponding λ_{fs} . The virial transfer function $T_v(a, k) = [1 + (k/k_v)^{\beta_v}]^{\gamma_v}$ is given in terms of the virial mode k_v and two constant parameters β_v and γ_v . We compare $T_v(a, k)$ with the Boltzmann code CLASS for WDM in the mass range 1-10 keV and we obtain the constraint $\beta_v\gamma_v = -18$ with $\nu = 1.020 \pm 0.025$. In the standard approach the transfer function is given by $T(a, k) = [1 + (\alpha k)^\beta]^\gamma$ [2] where α encodes the dynamical properties of WDM and must be numerically adjusted by means of a Boltzmann code. In contrast, in our virial approach the physical quantity k_v is simply given in terms of the free streaming scale λ_{fs} and can be analytically determined. Our virial proposal has a good agreement with CLASS and improves slightly the results from the standard transfer function. To conclude, we have proposed a new physically motivated transfer function $T_v(a, k)$ where the properties of WDM are encoded in the virial wave number k_v , is straightforward to determine and improves the prediction of WDM clustering properties.

Keywords: dark matter theory, power spectrum, galaxy clustering

¹Corresponding author

Contents

1	Introduction	1
2	Warm Dark Matter	2
2.1	Transfer Function: Standard Approach	3
2.2	Analysis with k_α mode	3
3	The Virial Model	4
3.1	Transfer Function: Virial Approach	5
3.2	Analysis with the Virial mode k_v	6
3.3	Comparing the two approaches	7
4	Free-streaming scale and Virial radius r_v	9
4.1	Free Streaming scale	9
4.2	Halo Mass Function	11
5	Summary and Conclusion	12

1 Introduction

The standard Λ CDM model has been a very successful model to describe our Universe and is consistent with cosmological observational evidence such as the cosmic microwave background (CMB) anisotropies [4], galaxy redshift surveys [5], type Ia Supernovae [6] reach to the conclusion that the content of the Universe is composed of 69% dark energy driving the accelerated expansion of the Universe, 31% matter whose clustering feature influence the large scale structure formation, corresponding to 27% Dark Matter (DM) and the remaining 4% is baryonic matter.

The nature of dark matter has received a great deal of attention in the last decade, due in part of the missing satellites in the universe, and the amount of structure at different scales and redshifts puts strong constraints on the nature of dark matter. In recent times the large surveys such as SDSS-IV [7] and in the near future, DESI [8] in the near future will have an important impact in determining the properties of dark energy (DE) and dark matter (DM). Despite the efforts in both particle physics and cosmology, the nature and composition of the DM are still unknown. Candidates for DM can be classified according to its velocity dispersion, v_{nr} , when the DM particle become non-relativistic (given by the scale factor a_{nr}). For thermal relics one can relate the mass of the WDM particle to a_{nr} . In this case DM is cold for mass larger than $m_{\text{cdm}} \sim \mathcal{O}(\text{MeV})$. This kind of DM particles stop being relativistic and start clustering object at early times. DM with a mass around $m_{\text{wdm}} \sim \mathcal{O}(\text{keV})$ are known to be warm, WDM, whose main attribute is that its dispersion velocity wipes out some density concentrations of matter and, therefore, induce a cut-off scale into the mass halo function [9]. The amount of energy density today Ω_{dmo} along with the scale factor when the WDM particle becomes non-relativistic a_{nr} are crucial for determining the properties of the large scale structure of the universe. For instance, the dispersion velocity of DM particles wipes out density concentrations of matter and, therefore, induce a cut-off scale in the mass halo function [9]. Most DM candidates have a smooth evolution of the DM velocity, however, phase

transitions in the underlying particle physics model for dark matter shows that an abrupt transition to a non-relativistic limit is plausible [10, 11].

The large velocity dispersion of DM at early stages on the evolution of the Universe tends to suppress gravitational clustering at small scales and conciliates with what it is observed. Cosmological N-body simulations of the Λ CDM model predict the number of satellite galaxies in Milky Way-like galaxies is smaller than the expected, the so-called missing satellite problem [12–14] and high concentrations of DM in the innermost regions of galaxies (cusp-core problem [15, 16]). Baryon physics also pursued the solutions to this problem by integrating star formation and halo evolution in the galaxy, however, the discussion is still in progress [17–19]. The details of the suppression at small scales depend on the DM particle nature, which takes us to connect the DM models and astrophysical observations. It can be determined by the parametrization of the transfer function $T_X(a, k) = (P_X/P_{cdm})^{1/2}$ in terms of the power spectrum of X DM particles and Λ CDM model, where T_X is scale and time-dependent. It has been conventional to compare the X and CDM models at the epoch when the amplitude of the fluctuations of model X is half the size of Λ CDM, i.e. $T_X(a, k)^2 = 1/2$. Different ansatzes have been proposed to parametrize the transfer function $T_X(a, k)$ and the parameters involved must be numerically fitted using numerical Boltzmann codes [2, 3].

Here, we will present a new approach to structure formation where the virial radius places a dominant role in structure formation. This new approach is physically motivated and is consistent with previous works in WDM structure formation and it allows for an understanding of the suppression of small scale structure in terms of the virial mass and radius. We introduce a new analytical transfer function, physically motivated, that reproduces the clustering of large classes non-thermal DM models and preserving the connection with the physics and nature of the DM.

We present and compare the standard and our virial transfer function in section 2.1 and section 3, and the free streaming scale in Section 4, the dark matter analysis and finally the conclusion in section 5.

2 Warm Dark Matter

The clustering properties of Dark Matter have a direct impact on the number of halo as a function of mass and redshift and can be contrasted with several observational large scale structure experiment as [7]. The velocity dispersion of DM particles plays a crucial role in structure formation. While DM particles are still relativistic, primordial density fluctuations are suppressed due to the velocity dispersion of DM particles and inhibit the formation of structure below the free streaming scale λ_{fs} [20]. Here, we will present two approaches to extract cosmological clustering properties of warm dark matter (WDM) in terms of Transfer Function $T(a, k)$ defined as the quotient of the linear matter perturbations between WDM and CDM. We refer to the standard approach the work of M. Viel et al. [2, 21] presented in section 2.1 while our virial approach is given in section 3.

Throughout this paper, we adopt Planck 2018 cosmological parameters [4] in a flat Universe with $\omega_{dmo} = 0.12$, and $\omega_{bo} = 0.02237$ as the CDM matter and baryonic with $\omega_i = \Omega_i h^2$ (with $i = dm, b$) and $h = 0.6736$ the Hubble constant in units of $100 \text{ km s}^{-1} \text{ Mpc}^{-1}$, $z_{\text{reio}} = 7.67$ the reionization redshift, $n_s = 0.965$ the tilt of the primordial power spectrum and $\ln(10^{10} A_s) = 3.044$ with A_s the amplitude of primordial fluctuations.

2.1 Transfer Function: Standard Approach

We will now present the standard approach to extract cosmological clustering properties of warm dark matter (WDM) using the Transfer Function defined as the quotient of the linear matter perturbations between WDM and CDM. The velocity dispersion of dark matter particles inhibits the formation of structure and the main parameter to account for this dispersion is the scale factor when these particles become non-relativist given by a_{nr} [20] and recently in [11]. The evolution of the linear energy density fluctuations are conveniently calculated by publicly available Boltzmann codes, e.g. CAMB [22] and CLASS [1], giving a power spectrum of matter-energy density fluctuations $P_{lin}(a, k)$. By comparing the power spectrum for different types of WDM particles one can infer the properties of a new WDM model without the need to implement the new model in the Boltzmann codes. The parametrization of the matter power spectrum for different WDM models has been presented in [2, 3], where the properties of WDM models can be studied employing the transfer function $T(a, k)$, defined as

$$T(a, k) = \left[\frac{P_{lin}^{wdm}(a, k)}{P_{lin}^{cdm}(a, k)} \right]^{1/2} \quad (2.1)$$

by comparing the power spectrum in the WDM model with CDM. The clustering properties of WDM are conveniently determined by the scale $k_{1/2}$ mode, where the power spectrum of the WDM model is suppressed by 50% compared to a Λ CDM model, i.e.

$$[T(a, k_{1/2})]^2 = \frac{1}{2} \quad (2.2)$$

and it is a convenient reference point, in Table 1 we show some $k_{1/2}$ values for different WDM models. The standard transfer function for thermal WDM particle is given by [2, 3, 20, 23, 24]

$$T(k) = [1 + (\alpha k)^\beta]^\gamma. \quad (2.3)$$

The clustering properties of the dark matter model is contained in α while β and γ are constant parameters to be fitted from numerical simulations. The quantity α has been estimated in [2, 3]

$$\alpha = 0.049 \left(\frac{m_{wdm}}{1keV} \right)^{1.11} \left(\frac{\Omega_{wdm}}{0.25} \right)^{0.11} \left(\frac{h}{0.7} \right)^{1.22} h^{-1} Mpc. \quad (2.4)$$

We can take β and γ as independent parameters or constrain them to be proportional to a single parameter μ as in [2] where they find

$$\beta = 2\mu, \quad \gamma = -5/\mu, \quad \mu = 1.12 \quad (2.5)$$

with $\beta\gamma = -10$.

2.2 Analysis with k_α mode

Alternatively to $k_{1/2}$, we can define the mode $k_\alpha \equiv 1/\alpha$ rendering $T(k_\alpha) = 2^\gamma$. From Eq.(2.3) we see that the half mode is proportional to $1/\alpha$

$$k_{1/2} = \frac{1}{\alpha} \left[\left(\frac{1}{\sqrt{2}} \right)^{1/\gamma} - 1 \right]^{1/\beta} = \frac{1}{\alpha} \xi_V \quad (2.6)$$

with a proportionality constant

$$\xi_V \equiv \left[\left(\frac{1}{\sqrt{2}} \right)^{1/\gamma} - 1 \right]^{1/\beta}. \quad (2.7)$$

For the values given in eq.(2.5) we obtain $\xi_V \simeq 0.36$. We define the mode

$$k_\alpha \equiv \frac{1}{\alpha} = \frac{k_{1/2}}{\xi_V} \quad (2.8)$$

and $k_\alpha > k_{1/2}$. We see that for $k = k_\alpha$ the transfer function takes the constant value

$$T(k_\alpha) = 2^\gamma \quad (2.9)$$

with $T(k_\alpha) \simeq 0.045$ for $\gamma = -5/\mu$, $\mu = 1.12$.

The ratio of the transfer function $T_X(k_\alpha)/T_X(k_{1/2}) \simeq 1/10$ but $k_\alpha/k_{1/2} \simeq 3$. Since k_α is larger than $k_{1/2}$ it corresponds to a less linear mode with a smaller transfer function $T_X(k_\alpha)$ indicating a larger deviation from Λ CDM model. The information using $T_X(k_{1/2}^V) = 1/2$ or $T_X(k_\alpha) = 2^\gamma$ and k_α is the same and k_α provides an alternative mode to compare WDM models using the transfer function.

3 The Virial Model

We propose to determine the transfer function $T_v(k_v)$ as a function of the virial mode k_v , defined in terms of the free streaming mode with $k_v = 2\pi/\lambda_v$ with $r_v = \lambda_v/2$ half the radius of as structure with a size of the free streaming scale λ_{fs} . We refer to the transfer function $T_v(k_v)$ as the virial approach. The free streaming scale λ_{fs} and mass M_{fs} are

$$\lambda_{fs}(t) \equiv \int_0^t \frac{v(a)dt'}{a(t')}, \quad M_{fs} = \left(\frac{4\pi r_{fs}^3}{3} \right) \rho_o, \quad (3.1)$$

with $r_{fs} = \lambda_{fs}/2$ and ρ_o present matter content of the universe. The virial mode, radius and virial mass are given by

$$k_v = 2\pi/\lambda_v, \quad r_v = \frac{\lambda_v}{2} = \frac{\lambda_{fs}}{4}, \quad M_v = (4\pi r_v^3/3) \rho_v. \quad (3.2)$$

The mass contained in the virialized structure is conserved and the virial mass is $M_v = M_{fs}$ and since r_v is half the size of r_{fs} the density of the virial sphere is $\rho_v = 8\rho_o$. Of course, a halo density profile such as NFW [25, 26] for example, would be more appropriate to determine the energy density inside this structure but this lies beyond the scope of this work. We take the transfer function for the virialized mode k_v as a two-parameter linear transfer function $T_v(k_v)$ as a function of the virial mode k_v , similar as the Standard Transfer,

$$T_v(k) = \left[1 + \left(\frac{k}{k_v} \right)^{\beta_v} \right]^{\gamma_v} \quad (3.3)$$

with β_v and γ_v constant parameters. We determine the values of these parameters in the next section (3), where we find that β_v and γ_v are correlated leaving $T_v(k)$ with only one free parameter.

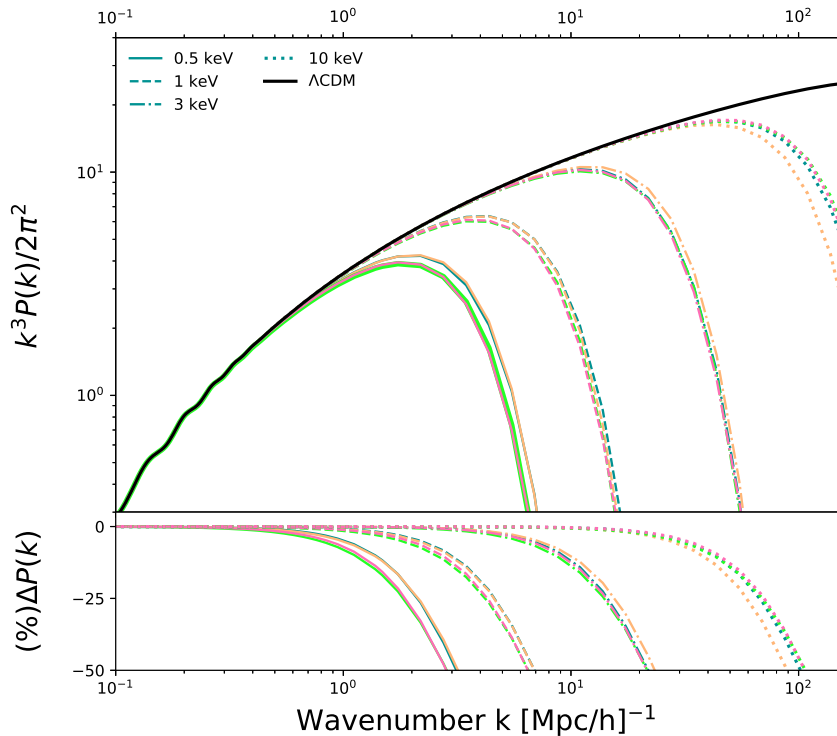


Figure 1: Top panel. Plots of linear dimensionless matter power spectra for the CDM (black solid line) and WDM of different masses, 0.5, 1, 3, and 10 keV, plotted as straight, dashed, dot-dashed and dotted lines, respectively. Dark green color lines are those obtained from CLASS. Orange color lines is the power spectrum is given from the parametrization, Eq.(2.3), pink and light green lines are the virial parametrization form Eqs. (3.7) and (3.9), respectively. We show the percentage difference, $\Delta P(k)$, with respect the CDM matter over spectrum.

3.1 Transfer Function: Virial Approach

Let us now determine compare the transfer function $T_v(k)$ with Boltzmann codes for different WDM models.

$$T_v(k) = \left[1 + \left(\frac{k}{k_v} \right)^{\beta_v} \right]^{\gamma_v} \quad (3.4)$$

with β_v and γ_v constant parameters. All the physical properties of WDM are imprinted in the virial mode k_v which is directly related to the free-streaming scale λ_{fs} given in eq.(4.7) and it is not adjusted by the Boltzmann codes, contrary to the α parameter in eq.(2.4) in section 2.1. The dependence of k in the transfer function in eq.(3.3) is given by

$$\frac{k}{k_v} = \frac{r_v}{r} \quad (3.5)$$

The scale $k = k_v = 2k_{fs}$ corresponds to a radius r_v which is half the size of the free streaming scale radius $r_{fs} = \lambda_{fs}/2$. We therefore have virial radius and k mode

$$r_v \equiv \frac{r_{fs}}{2} = \frac{\lambda_{fs}}{4}, \quad k_v = 2k_{fs} = \frac{4\pi}{\lambda_{fs}}. \quad (3.6)$$

The dependence of the transfer function on the mass of the WDM particle is in the virial mode, k_v , and not in the α parameters of the transfer function as in eq.(3.3). The mode k_v can be easily determined since it is proportional to the free streaming scale (cf. eq.(4.1)) and does not require to be fitted using a numerical Boltzmann code. To determine the values of β_v and γ_v we compare our transfer virial function with WDM models from Class code [1], see Fig.2.

We found numerically convenient to define the parameters β_v and γ_v as $\beta_v = 2\nu$ and $\gamma_v = -\zeta/\nu$ and we take ζ and ν as the independent parameters and we obtain for WDM masses in the range (1-10)keV using CLASS, using the result for a_{nr} given in eq.(4.10) to compute λ_{fs} and $k_v = 4\pi/\lambda_{fs}$,

$$T = \left(1 + \left(\frac{k}{k_v} \right)^{2\nu} \right)^{-\zeta/\nu}. \quad (3.7)$$

$$\beta_v = 2\nu, \quad \gamma_v = -\zeta/\nu, \quad \nu = 1.0253 \pm 0.0232, \quad \zeta = 9.17 \pm 0.19. \quad (3.8)$$

giving a constraint $\beta_v\gamma_v = -2\zeta = 18.34 \pm 0.38$. We also consider the case with a single free parameter, as in the standard approach, by relating β_v and γ_v . Contrary to the ansatz in the standard transfer function approach, here we choose to define $\beta_v = 2\nu$ and $\gamma_v = -9/\nu$ giving a constraint $\gamma_v\beta_v = -18$

$$T = \left(1 + \left(\frac{k}{k_v} \right)^{2\nu} \right)^{-9/\nu} \quad (3.9)$$

with

$$\beta_v = 2\nu, \quad \gamma_v = -9/\nu, \quad \nu = 1.020 \pm 0.025. \quad (3.10)$$

Notice that the value of ν in the one parameter case in eq.(3.10) is consistent with the two parameters in eq.(3.8) and allowing us to work with the transfer function in eq.(3.9).

In Table 1 and Fig.2 and Fig.1 we show how good the virial transfer functions is by computing the $k_{1/2}$ for different models, for the standard transfer function, $k_{1/2}^{\text{viel}}$, and also the virial approach with 2 free parameters, eq.(3.7) denoted as $k_{1/2}^{2p}$ and with 1 free parameter, eq.(3.9) and denoted as $k_{1/2}^{1p}$. The numbers in parenthesis are the percentage difference in comparison with the scale directly obtained from the numerical solution from CLASS, $k_{1/2}^{\text{class}}$. Class code [1], see Fig.2. We show in table 2 the values of k_v , r_v , M_v and a_{nr} for different WDM masses in the range 1-10keV in our virial approach.

3.2 Analysis with the Virial mode k_v

For $k = k_v$ the transfer function takes the value $T_X(k) = (2)^{\gamma_v}$, independently of the value of β_v , and can be used to compare different DM models as k_α (c.f. eq.(2.8)) given in the standard approach. From eq.(3.3) the half mode $k_{1/2}^v$ (i.e. $T_v^2(k_{1/2}^v) = 1/2$) is given by

$$k_{1/2}^v = k_v \xi_v \quad (3.11)$$

with

$$\xi_v \equiv \left[\left(\frac{1}{\sqrt{2}} \right)^{1/\gamma_v} - 1 \right]^{1/\beta_v} \quad (3.12)$$

with a constant value given by $\xi_v \simeq 0.21$ using eq.(3.10).

Mass	a_{nr}	k_v	$k_{1/2}^{v1p}$	$k_{1/2}^{v2p}$	$k_{1/2}^{viel}$	$k_{1/2}^{class}$
1 keV	1.20×10^{-7}	31.58	6.53 (5.60%)	6.53 (5.60%)	6.92 (0.11%)	6.91
2 keV	4.97×10^{-8}	69.78	14.40 (4.40%)	14.47 (4.88%)	14.93 (8.25%)	13.79
3 keV	3.18×10^{-8}	104.98	21.64 (1.03%)	21.73 (0.58%)	23.37 (6.88%)	21.86
4 keV	1.98×10^{-8}	161.82	33.40 (3.60%)	33.40 (3.60%)	32.21 (7.03%)	34.65
5 keV	1.39×10^{-8}	223.48	46.26 (6.05%)	46.26 (6.05%)	41.31 (5.29%)	43.62
6 keV	1.09×10^{-8}	280.32	58.00 (5.61%)	58.00 (5.61%)	50.41 (8.20%)	54.91
7 keV	8.83×10^{-9}	339.04	70.13 (1.44%)	70.13 (1.44%)	59.86 (13.41%)	69.13
8 keV	7.39×10^{-9}	399.62	82.53 (5.17%)	82.53 (5.17%)	69.50 (20.15%)	87.03
9 keV	6.31×10^{-9}	461.86	95.39 (9.60%)	95.39 (9.60%)	79.24 (8.95%)	87.03
10 keV	5.56×10^{-9}	519.30	107.29 (2.08%)	107.29 (2.08%)	89.13 (18.65%)	109.57

Table 1: Viral wavenumbers k_v and $k_{1/2}$ for different transfer functions in hMpc^{-1} units. Values for $k_{1/2}^{v1p}$ and $k_{1/2}^{v2p}$ are obtained by the transfer function given by eq.(3.9) and eq.(3.7), respectively, while $k_{1/2}^{viel}$ is obtained from eq.(2.3). The values of a_{nr} and $k_{1/2}^{class}$, 2nd and last column respectively, were obtained from the transfer function given by the code CLASS.

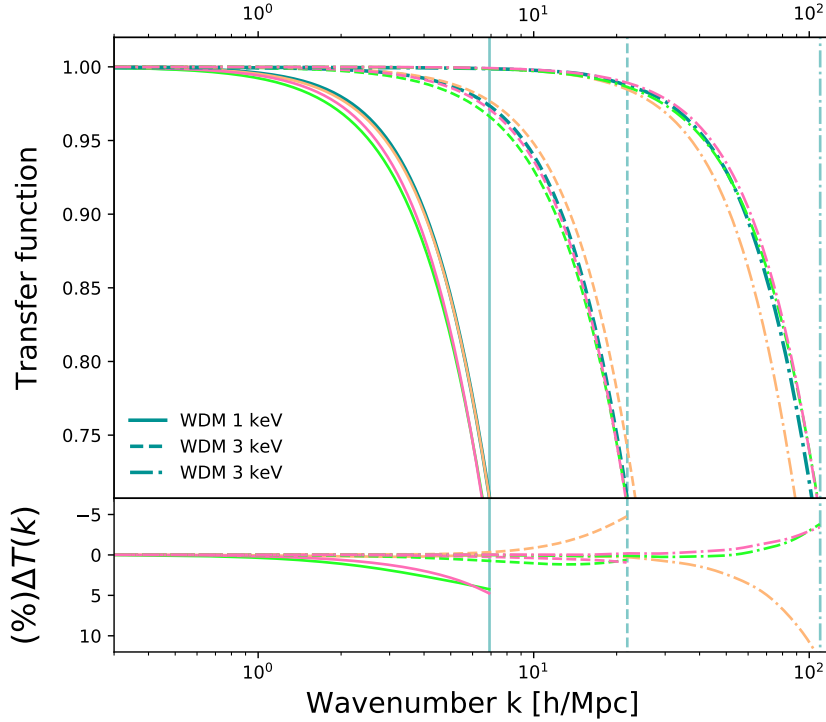


Figure 2: Transfer function for WDM. Solid, dashed, and dot-dashed lines represent WDM masses of 1, 3, and 10 keV, respectively. Dark green color are transfer functions from CLASS code, orange color are the transfer functions from Viel et al. [2] Eq.(2.3), pink lines are the virial transfer functions with 2 free parameter (Eq.3.7), and green lines is the transfer function with 1 free parameter (Eq.3.9).

3.3 Comparing the two approaches

We have presented an alternative approach to the Transfer function. In the standard transfer function approach in section 2.1 the quantity α given in eq.(2.4) contains the properties of DM model such as its mass (which can be related to the scale factor when it becomes

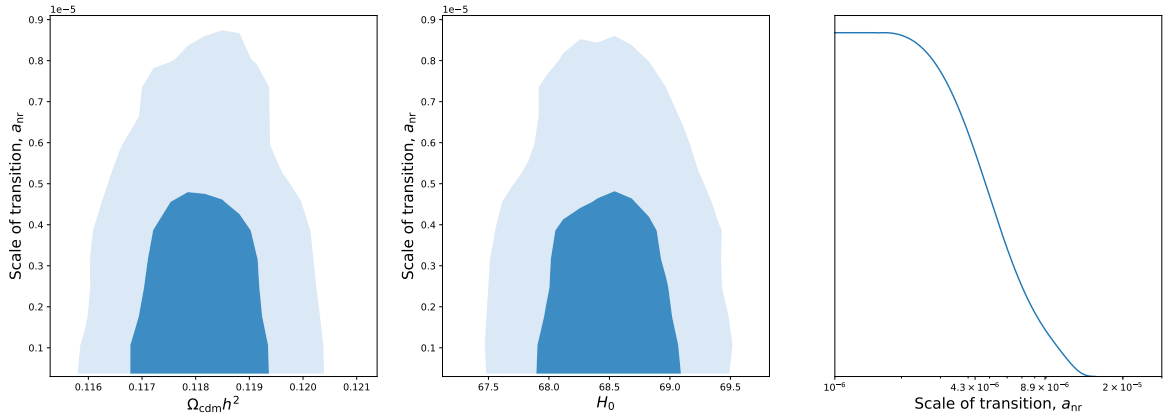


Figure 3: We show recent constrains [27] to a_{nr} from posterior probabilities at 68% and 95% confidence level in the parameter space $a_{nr} - \Omega_{\text{cdm}}$ (left), $a_{nr} - H_0$ (middle), and the marginalized posterior distribution of a_{nr} (right) using Planck EE, TE, and TT high- ℓ spectra [4] combined with Wigglez matter power spectrum [28] observations. At 1σ confidence level, the lower value is given by $a_{nr} < 4.3 \times 10^{-6}$.

Mass	a_{nr}	r_v	k_v	M_v
1 keV	1.20×10^{-7}	99.8	31.5	1.32×10^9
2 keV	4.76×10^{-8}	43.3	72.6	1.07×10^8
3 keV	2.77×10^{-8}	26.4	118.8	2.45×10^7
4 keV	1.89×10^{-8}	18.6	168.7	8.56×10^6
5 keV	1.40×10^{-8}	14.2	221.5	3.78×10^6
6 keV	1.10×10^{-8}	11.3	276.9	1.93×10^6
7 keV	8.96×10^{-9}	9.4	334.6	1.10×10^6
8 keV	7.50×10^{-9}	8.0	394.2	6.70×10^5
9 keV	6.41×10^{-9}	6.9	455.6	4.34×10^5
10 keV	5.57×10^{-9}	6.1	518.7	2.94×10^5

Table 2: Virial quantities for different WDM masses, with a_{nr} the scale factor of the WDM transition given by Eq.(4.10), r_v the virial radius in kpc/h is given from Eq.(3.6), the wave number k_v in $\text{Mpc}^{-1}h$, and the virial mass M_v in M_\odot/h^3 .

non-relativistic a_{nr} for thermal WDM particles), however the numerical values α have been numerically fitted using a Boltzmann code [2]. In our virial approach, all model dependence is encoded in the free-streaming scale λ_{fs} , which is well defined function and is not numerically fitted.

We plot the Matter Power Spectrum and the transfer functions in Fig.1 in the mass range (1 - 10) keV for WDM. Notice that the standard error for all three parameters are small, specially for α_v and β_v . The value of $\beta_v = 2.04$ is actually close to previous works that obtained $\beta = 2.24$ [2], however we find a significantly difference with $\gamma_v = -2.68$ compared to $\gamma = -4.46$. The difference in these parameters is because we take a different reference mode k_v instead of $k_\alpha = 1/\alpha$ as in Viel et al. [2] with similar proportionality constants $\xi_v = 0.21$ and $\xi_V = 0.36$.

Our transfer function is physically motivated and is determined in terms of the virial mode k_v which has a clear interpretation in terms of the free streaming scale and in contrast with the fitted α parameter (c.f. eq.(2.4)) in the standard approach [2, 3]. Our transfer

function has an excellent agreement once we compare with the Boltzmann numerical code, CLASS and it out performs the standard Transfer function in eq.(2.3) for massive particles in the range 1-10keV .

4 Free-streaming scale and Virial radius r_v

The thermal velocities of the dark matter particles have a direct influence on structure formation. While DM particles are still relativistic, primordial density fluctuations are suppressed on scales of order the Hubble horizon at that time. This is called the free-streaming scale and depends on the time when a massive particle becomes non-relativistic t_{nr} . It is defined by

$$\lambda_{fs}(t) \equiv \int_0^t \frac{v(a)dt'}{a(t')} \quad (4.1)$$

The corresponding free-streaming scale mode k_{fs} and a mass M_{fs} contained in sphere of radius $\lambda_{fs}/2$ are given by

$$k_{fs} = \frac{2\pi}{\lambda_{fs}}, \quad M_{fs} = \frac{4\pi}{3} \left(\frac{\lambda_{fs}}{2} \right)^3 \rho_{mo}. \quad (4.2)$$

and in terms of the virial mode

$$r_v = \frac{r_{fs}}{2} = \frac{\lambda_{fs}}{4}, \quad M_v = \left(\frac{4\pi r_v^3}{3} \right). \quad (4.3)$$

with $\rho_v = 8\rho_{mo}$. For mass-scales $M \lesssim M_v$ the free-streaming of particles erases all peaks in the initial density field therefore the number of structures below this mass scale should be significantly reduced in numbers. We show this behavior in Fig. 4, where we compare CDM and WDM mass functions. However, it is the virialized scale that accounts for the mass contained within the structure to be formed.

4.1 Free Streaming scale

It is conventional to report the free streaming scale assuming a relativistic regime with $v_{\text{wdm}} = c = 1$ for $a < a_{nr}$ and following a non-relativistic regime ($a > a_{nr}$) with $v_{\text{wdm}} = a_{nr}/a$. With these choices of v one gets the free streaming scale

$$\lambda_{fs}(t_{eq}) \simeq \int_0^{t_{nr}} \frac{cdt}{a(t)} + \int_{t_{nr}}^{t_{eq}} \frac{v_{\text{wdm}}dt}{a(t)}, \quad (4.4)$$

$$= \frac{2t_{nr}}{a_{nr}} \left[1 + \ln \left(\frac{a_{eq}}{a_{nr}} \right) \right] \quad (4.5)$$

to be compared with of Eq.(4.7) or its limit eq.(4.8). However, we prefer to follow our previous approach [11, 27] and define the time when a particle stops being relativistic, at scale factor a_{nr} , when $p^2 = m^2$ with p the momentum of the particles. The velocity in an expanding universe evolves as

$$v(a) = \frac{(a_{nr}/a)}{\sqrt{1 + (a_{nr}/a)^2}}, \quad (4.6)$$

which gives a velocity $v_{\text{wdm}}^2(a_{nr}) = 1/2$. Eq.(4.6) describes the exact velocity evolution of a decoupled massive particle. The transition between relativistic to non-relativistic is smooth

and continuous, see [11] for a generalize transition. This evolution is general and valid for any massive decoupled particles (WDM, CDM or massive neutrinos). Using eq.(4.6) in eq.(4.5) we get [11])

$$\lambda_{fs}(a_{eq}) = \frac{2t_{nr}}{a_{nr}} \ln \left[\frac{a_{eq}}{a_{nr}} + \sqrt{1 + \left(\frac{a_{eq}}{a_{nr}} \right)^2} \right], \quad (4.7)$$

which gives free streaming scale without approximation. However, for presentation purposes let assume that $a_{nr} \ll a_{eq}$ and then

$$\lambda_{fs}(a_{eq}) \simeq \frac{2t_{nr}}{a_{nr}} \left[\ln(2) + \ln \left(\frac{a_{eq}}{a_{nr}} \right) \right]. \quad (4.8)$$

Here, we use in our calculations eq.(4.7) but for presentation purposes we take the approximations in eq.(4.8). We express $2t_{nr} = 1/H_{nr}$ and $H_{nr} = (a_{eq}/a_{nr})^2 (a_o/a_{eq})^{3/2} H_o$ to obtain

$$\frac{2t_{nr}}{a_{nr}} = 0.011 \left(\frac{1 + z_{eq}}{1 + 3411} \right)^{1/2} \left(\frac{a_{nr}}{2.77 \times 10^{-8}} \right) \frac{\text{Mpc}}{\text{h}} \quad (4.9)$$

where a_{nr} has been previously computed in [11],

$$\frac{a_{nr}}{a_o} = 2.77 \times 10^{-8} \left(\frac{\Omega_{dmo} h^2}{0.120} \right)^{1/3} \left(\frac{3 \text{ keV}}{m_{\text{wdm}}} \right)^{4/3}, \quad (4.10)$$

where we consider the DM particle as a fermion with $g_f = 7/4$ degrees of freedom. With a simple analytic approach for a massive particles characterized by having a non-negligible thermodynamic velocity dispersion [2, 20, 23, 24, 29–37] we can compute the fluid approximation for the perturbation equations for any massive particles, given the analytic solution for the energy density evolution we were able to reproduce the most appealing feature of WDM, the cut-off in the matter power spectrum [2, 3, 23, 24]. The percentage difference between the numerical value obtained from Boltzmann equations and the analytic one of a_{nr} is on average 3% in a mass range 1-10 keV.

In Table 2 we show different values of a_{nr} and in Fig. 3 we show the lower limits that constrains a_{nr} from the fluid approximation [27] applied to WDM. The free-streaming scale λ_{fs} and mass in the limit $a_{nr}/a_{eq} \ll 1$ take the following values

$$\lambda_{fs} \simeq 97.0 \left(1 + \left(\frac{1}{8.82} \right) \left(\frac{1 + 3411}{1 + z_{eq}} \right) \left(\frac{2.77 \times 10^{-8}}{a_{nr}} \right) \right) \frac{\text{kpc}}{\text{h}} \quad (4.11)$$

with $\lambda_{fs} = 108.2 \text{ kpc/h}$ for $z_{eq} = 3411$, $a_{nr} = 2.77 \times 10^{-8}$, and a contained mass of

$$M_{fs}^{\text{wdm}} = 2.45 \times 10^7 \left(\frac{\Omega_{dmo} h^2}{0.12} \right) \left(\frac{\lambda_{fs}}{108.2 \text{ kpc}} \right)^3 M_{\odot}.$$

The virialized structure has a mass $M_v = M_{fs}$, however the energy density in the virialized structure is eight times larger than in M_{fs} , and a radius $r_v = r_{fs}/2 = \lambda_{fs}/4$ with

$$r_v = 24.25 \left(1 + \left(\frac{1}{8.82} \right) \left(\frac{1 + 3411}{1 + z_{eq}} \right) \left(\frac{2.77 \times 10^{-8}}{a_{nr}} \right) \right) \frac{\text{kpc}}{\text{h}} \quad (4.12)$$

$$= 26.4 \left(\frac{\lambda_{fs}}{108.2 \text{ kpc/h}} \right) \frac{\text{kpc}}{\text{h}}. \quad (4.13)$$

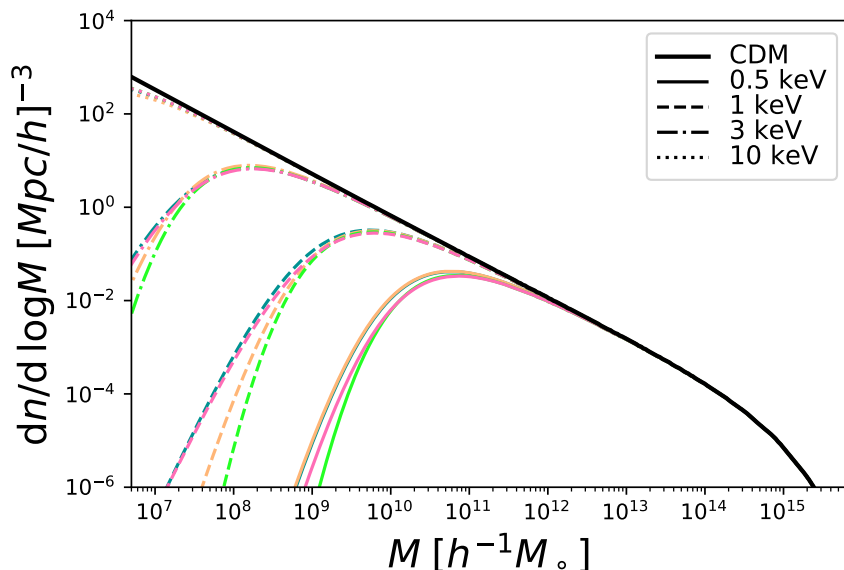


Figure 4: Plot of the halo mass function. The black solid line is the CDM model; Color straight, dashed, dot-dashed and dotted line styles represent 0.5, 1, 3, and 10 keV WDM masses respectively. Color lines represent the halo mass function from different matter power spectrum. Dark green are the lines from CLASS, pink and light green lines are the virial parametrization form Eqs. (3.7) and (3.9), respectively. And orange color lines is the standard parametrization, Eq.(2.3).

4.2 Halo Mass Function

The comoving number density of collapsed structure is computed using the Press-Schechter formalism [38]. With the linear matter power spectrum obtained from the transfer function, eq.(2.1), we compute the halo mass function having mass range M to $M + dM$ as

$$\frac{dn}{d \log M} = \frac{1}{2} \frac{\bar{\rho}}{M} \mathcal{F}(\nu) \frac{d \log \sigma^2}{d \log M} \quad (4.14)$$

where n is the number density of haloes, M the halo mass and the peak-height of perturbations is given by $\nu = \frac{\delta_c^2(z)}{\sigma^2(M)}$, where $\delta_c = 1.686$ is the critical overdensity required for a structure to collapse in a dark matter halo in the Λ CDM cosmology. The average matter density is $\bar{\rho}$. The corresponding variance of the smoothed density fluctuation in a sphere of radius R enclosing a mass M is $\sigma^2(M)$, can be computed from the following integrals

$$\sigma^2(M) = \int_0^\infty dk \frac{k^2 P_{\text{lin}}(k)}{2\pi^2} |W(kR)|^2. \quad (4.15)$$

Here we will use the sharp-k window function $W(x) = \Theta(1 - kR)$, with Θ being a Heaviside step function (smoothes the large scale mass distribution to a continuous density field), and $R = (3cM/4\pi\bar{\rho})^{1/3}$, where the value of $c = 2.5$ is proved to be best for cases similar as the WDM [39]. Finally, for the mass function, $\mathcal{F}(\nu)$, we adopt [40] that is giving as

$$\mathcal{F}(\nu) = A \left(1 + \frac{1}{\nu^p} \right) \sqrt{\frac{\nu'}{2\pi}} e^{-\nu'/2} \quad (4.16)$$

with $\nu' = 0.707\nu$, $p = 0.3$, and $A = 0.322$ determined from the integral constraint $\int f(\nu) d\nu = 1$.

Using the matter power spectrum using the transfer function with Eq.(2.1), and using the virial approach Eqd.(3.9) and (3.7). We compute the halo mass function, see Fig.4, and compare it with the mass function obtained from CLASS numerical solutions to the matter power spectrum and the same from Viel transfer function, Eq.(2.3).

5 Summary and Conclusion

We studied the clustering properties of WDM particles and we present the virial approach, where the transfer function depends on the virial wave number $k_v = 4\pi/\lambda_{fs}$, and we compare it to the standard approach. The velocity dispersion of WDM at early stages on the evolution of the universe suppress gravitational clustering and may conciliates observations of the number of small scales galaxies. The details of the suppression depend on the properties of the DM particles, however a key ingredient is the time when these particles become non-relativist given by the scale factor a_{nr} .

We have presented here a new approach to structure formation where the virial radius r_v places a dominant role. The virial mode k_v is defined in terms of the free streaming scale λ_{fs} and depends thus directly on a_{nr} . This new approach is physically motivated, is consistent with previous works in WDM structure formation, and allows for an understanding the suppression of small scale structure in terms of the virial mass and radius, M_v and r_v respectively. The transfer function $T(a, k)$ is determined in terms of the virial mode k_v which has a clear interpretation in terms of the free streaming scale and is easily calculated, contrasting with the α parameter of eq.(2.4) [2, 3] which requires a numerical fit.

From Table (1) we see that our virial transfer function performs better than the standard transfer function for WDM with masses in the range (1-10) keV. The standard transfer function has up to two constant parameters (β, γ) which can be reduced to only one μ with $\beta = 2\mu$, $\gamma = -5/\mu$ with $\mu = 1.12$ supplemented by the α containing the relevant clustering parameters of the WDM model in eq.(2.4) and has been fitted to give the correct value of $k_{1/2}$ for different WDM models. Since α has been numerically fitted we consider it as a free parameter. Therefore the standard transfer function has up to three parameters and can be reduced to two parameters by taking the fitted constraint $\gamma\beta = -10$. On the other hand our virial Transfer function parametrization in eq.(3.7) has only two parameters β, γ . As in the Standard Transfer function we can reduce a parameter by taking $\gamma_v\beta_v$ constant. Doing so, we found $\beta_v = 2\nu$, $\gamma_v = -9/\nu$ with $\nu = 1.09$, and $\gamma_v\beta_v = -18$. Taking β_v and γ_v independent we obtained $\beta_v = 2.05 \pm 0.04$, $\gamma_v = -8.94 \pm 0.10$ with $\gamma_v\beta_v = -18.32$ at the central values. Clearly the one and two parameter Transfer Function in the virial approach are consistent. We obtained for a WDM thermal particle that becomes non-relativistic at $a_{nr} = 2.77 \times 10^{-8}$, corresponding to a 3 keV mass, a virial radius $r_v = 26.4M_{pc}$ with wave number $k_v = 21.64$ in the virial approach and a $k_{1/2} = 21.86$ in the standard approach, corresponding to a structure with a contained mass of $\mathcal{O}(10^7) M_\odot$.

We have shown that our virial parametrization of the transfer function is physically motivated and has an excellent agreement with numerical results from Boltzmann CLASS codes shown in Table (1) and Fig.(2) and Fig.(1) and outperforming slightly the standard transfer function [2, 20] given in eq.(2.3) for masses in the range 1-10 keV. The parameter α in the Standard Transfer function must be fitted numerically using Boltzmann code, while in our approach the physical parameter $k_v = 2k_{fs}$ is determined in terms of the free streaming mode λ_{fs} an easily computed quantity.

Acknowledgments

AM acknowledges partial support from Project IN103518 PAPIIT-UNAM, PASPA DGAPA-UNAM and CONACyT. JM acknowledges Catedras-CONACyT financial support and MCT-P/UNACH as the hosting institution of the Catedras program.

References

- [1] Julien Lesgourgues. The Cosmic Linear Anisotropy Solving System (CLASS) I: Overview. 4 2011.
- [2] Matteo Viel, Julien Lesgourgues, Martin G. Haehnelt, Sabino Matarrese, and Antonio Riotto. Constraining warm dark matter candidates including sterile neutrinos and light gravitinos with WMAP and the Lyman-alpha forest. *Phys. Rev.*, D71:063534, 2005. doi: 10.1103/PhysRevD.71.063534.
- [3] Matteo Viel, George D. Becker, James S. Bolton, and Martin G. Haehnelt. Warm dark matter as a solution to the small scale crisis: New constraints from high redshift Lyman- α forest data. *Phys. Rev. D*, 88:043502, 2013. doi: 10.1103/PhysRevD.88.043502.
- [4] N. Aghanim et al. Planck 2018 results. VI. Cosmological parameters. 2018.
- [5] T. Abbott et al. The Dark Energy Survey: more than dark energy ? an overview. *Mon. Not. Roy. Astron. Soc.*, 460(2):1270–1299, 2016. doi: 10.1093/mnras/stw641.
- [6] M. Betoule et al. Improved cosmological constraints from a joint analysis of the SDSS-II and SNLS supernova samples. *Astron. Astrophys.*, 568:A22, 2014. doi: 10.1051/0004-6361/201423413.
- [7] Shadab Alam et al. The Completed SDSS-IV extended Baryon Oscillation Spectroscopic Survey: Cosmological Implications from two Decades of Spectroscopic Surveys at the Apache Point observatory. 7 2020.
- [8] Michael E. Levi et al. The Dark Energy Spectroscopic Instrument (DESI). 7 2019.
- [9] Maria Archidiacono and Steen Hannestad. Updated constraints on non-standard neutrino interactions from Planck. *JCAP*, 1407:046, 2014. doi: 10.1088/1475-7516/2014/07/046.
- [10] A. de la Macorra. BDM Dark Matter: CDM with a core profile and a free streaming scale. *Astropart.Phys.*, 33:195–200, 2010. doi: 10.1016/j.astropartphys.2010.01.009.
- [11] Jorge Mastache and Axel de la Macorra. Bound Dark Matter (BDM) towards solving the Small Scale Structure Problem. *JCAP*, 2003(03):025, 2020. doi: 10.1088/1475-7516/2020/03/025.
- [12] Stelios Kazantzidis, Lucio Mayer, Chiara Mastropietro, Jurg Diemand, Joachim Stadel, and Ben Moore. Density profiles of cold dark matter substructure: Implications for the missing satellites problem. *Astrophys. J.*, 608:663–3679, 2004. doi: 10.1086/420840.
- [13] Michael Boylan-Kolchin, James S. Bullock, and Manoj Kaplinghat. Too big to fail? The puzzling darkness of massive Milky Way subhaloes. *Mon. Not. Roy. Astron. Soc.*, 415:L40, 2011. doi: 10.1111/j.1745-3933.2011.01074.x.
- [14] Anatoly A. Klypin, Andrey V. Kravtsov, Octavio Valenzuela, and Francisco Prada. Where are the missing Galactic satellites? *Astrophys. J.*, 522:82–92, 1999. doi: 10.1086/307643.
- [15] Jorge Mastache, Axel de la Macorra, and Jorge L. Cervantes-Cota. Core-Cusp revisited and Dark Matter Phase Transition Constrained at $O(0.1)$ eV with LSB Rotation Curve. *Phys. Rev.*, D85:123009, 2012. doi: 10.1103/PhysRevD.85.123009.
- [16] David J. E. Marsh and Ana-Roxana Pop. Axion dark matter, solitons and the cusp-core problem. *Mon. Not. Roy. Astron. Soc.*, 451(3):2479–2492, 2015. doi: 10.1093/mnras/stv1050.

- [17] Shea Garrison-Kimmel et al. Not so lumpy after all: modelling the depletion of dark matter subhaloes by Milky Way-like galaxies. *Mon. Not. Roy. Astron. Soc.*, 471(2):1709–1727, 2017. doi: 10.1093/mnras/stx1710.
- [18] Till Sawala et al. The APOSTLE simulations: solutions to the Local Group’s cosmic puzzles. *Mon. Not. Roy. Astron. Soc.*, 457(2):1931–1943, 2016. doi: 10.1093/mnras/stw145.
- [19] Marcel S. Pawlowski, Benoit Famaey, David Merritt, and Pavel Kroupa. On the persistence of two small-scale problems in Λ CDM. *Astrophys. J.*, 815(1):19, 2015. doi: 10.1088/0004-637X/815/1/19.
- [20] Paul Bode, Jeremiah P. Ostriker, and Neil Turok. Halo formation in warm dark matter models. *Astrophys. J.*, 556:93–107, 2001. doi: 10.1086/321541.
- [21] Matteo Viel, George D. Becker, James S. Bolton, and Martin G. Haehnelt. Warm dark matter as a solution to the small scale crisis: New constraints from high redshift Lyman-alpha forest data. *Phys. Rev.*, D88:043502, 2013. doi: 10.1103/PhysRevD.88.043502.
- [22] Antony Lewis and Sarah Bridle. Cosmological parameters from CMB and other data: A Monte Carlo approach. *Phys. Rev. D*, 66:103511, 2002. doi: 10.1103/PhysRevD.66.103511.
- [23] Pedro Colin, Vladimir Avila-Reese, and Octavio Valenzuela. Substructure and halo density profiles in a warm dark matter cosmology. *Astrophys. J.*, 542:622–630, 2000. doi: 10.1086/317057.
- [24] Steen H. Hansen, Julien Lesgourgues, Sergio Pastor, and Joseph Silk. Constraining the window on sterile neutrinos as warm dark matter. *Mon. Not. Roy. Astron. Soc.*, 333:544–546, 2002. doi: 10.1046/j.1365-8711.2002.05410.x.
- [25] Julio F. Navarro, Carlos S. Frenk, and Simon D. M. White. The Structure of cold dark matter halos. *Astrophys. J.*, 462:563–575, 1996. doi: 10.1086/177173.
- [26] Julio F. Navarro, Carlos S. Frenk, and Simon D. M. White. A Universal density profile from hierarchical clustering. *Astrophys. J.*, 490:493–508, 1997. doi: 10.1086/304888.
- [27] Jorge Mastache and Axel de la Macorra. Analytic Fluid Approximation for Warm Dark Matter. 9 2019.
- [28] David Parkinson et al. The WiggleZ Dark Energy Survey: Final data release and cosmological results. *Phys. Rev. D*, 86:103518, 2012. doi: 10.1103/PhysRevD.86.103518.
- [29] Scott Dodelson and Lawrence M. Widrow. Sterile-neutrinos as dark matter. *Phys. Rev. Lett.*, 72:17–20, 1994. doi: 10.1103/PhysRevLett.72.17.
- [30] A. D. Dolgov and S. H. Hansen. Massive sterile neutrinos as warm dark matter. *Astropart. Phys.*, 16:339–344, 2002. doi: 10.1016/S0927-6505(01)00115-3.
- [31] Takehiko Asaka, Mikko Laine, and Mikhail Shaposhnikov. Lightest sterile neutrino abundance within the nuMSM. *JHEP*, 01:091, 2007. doi: 10.1088/1126-6708/2007/01/091,10.1007/JHEP02(2015)028. [Erratum: *JHEP*02,028(2015)].
- [32] Xiang-Dong Shi and George M. Fuller. A New dark matter candidate: Nonthermal sterile neutrinos. *Phys. Rev. Lett.*, 82:2832–2835, 1999. doi: 10.1103/PhysRevLett.82.2832.
- [33] Kevork Abazajian, George M. Fuller, and Mitesh Patel. Sterile neutrino hot, warm, and cold dark matter. *Phys. Rev.*, D64:023501, 2001. doi: 10.1103/PhysRevD.64.023501.
- [34] Alexander Kusenko. Sterile neutrinos, dark matter, and the pulsar velocities in models with a Higgs singlet. *Phys. Rev. Lett.*, 97:241301, 2006. doi: 10.1103/PhysRevLett.97.241301.
- [35] Kalliopi Petraki and Alexander Kusenko. Dark-matter sterile neutrinos in models with a gauge singlet in the Higgs sector. *Phys. Rev.*, D77:065014, 2008. doi: 10.1103/PhysRevD.77.065014.

- [36] Alexander Merle and Maximilian Totzauer. keV Sterile Neutrino Dark Matter from Singlet Scalar Decays: Basic Concepts and Subtle Features. *JCAP*, 1506:011, 2015. doi: 10.1088/1475-7516/2015/06/011.
- [37] Johannes König, Alexander Merle, and Maximilian Totzauer. keV Sterile Neutrino Dark Matter from Singlet Scalar Decays: The Most General Case. *JCAP*, 1611(11):038, 2016. doi: 10.1088/1475-7516/2016/11/038.
- [38] William H. Press and Paul Schechter. Formation of galaxies and clusters of galaxies by selfsimilar gravitational condensation. *Astrophys. J.*, 187:425–438, 1974. doi: 10.1086/152650.
- [39] Andrew J. Benson, Arya Farahi, Shaun Cole, Leonidas A. Moustakas, Adrian Jenkins, Mark Lovell, Rachel Kennedy, John Helly, and Carlos Frenk. Dark Matter Halo Merger Histories Beyond Cold Dark Matter: I - Methods and Application to Warm Dark Matter. *Mon. Not. Roy. Astron. Soc.*, 428:1774, 2013. doi: 10.1093/mnras/sts159.
- [40] J. R. Bond, S. Cole, G. Efstathiou, and Nick Kaiser. Excursion set mass functions for hierarchical Gaussian fluctuations. *Astrophys. J.*, 379:440, 1991. doi: 10.1086/170520.